Iterative calibration of a shape memory alloy constitutive model from 1D and 2D data using optimization methods

Daniel Whitten, Darren Hartl

Daniel Whitten, Darren Hartl, "Iterative calibration of a shape memory alloy constitutive model from 1D and 2D data using optimization methods," Proc. SPIE 9058, Behavior and Mechanics of Multifunctional Materials and Composites 2014, 905804 (9 March 2014); doi: 10.1117/12.2046666

SPIE.

Event: SPIE Smart Structures and Materials + Nondestructive Evaluation and Health Monitoring, 2014, San Diego, California, United States

Iterative Calibration of a Shape Memory Alloy Constitutive Model from 1-D and 2-D Data Using Optimization Methods

Daniel Whitten[a] and Darren Hartl[b,c]

[a]Dept. of Mechanical Engineering, Texas A&M University;
[b]Dept. of Aerospace Engineering, Texas A&M University;
[c]Texas Institute for Intelligent Material Systems and Structures, Texas A&M University

ABSTRACT

Shape memory alloy constitutive models have been shown to accurately predict 1-D and 3-D material response under general thermomechanical loading. As with any constitutive model, however, the degree to which simulation results match experimental data is dependent on the accurate calibration of model parameters. This work presents a general framework for the identification of SMA material parameters using numerical optimization methods and experimental results that include both 1-D data (i.e., stress-strain and strain-temperature line plots) as well as 2-D digital image correlation (DIC) strain field data. The optimization framework is verified using 1-D and 3-D finite-element-based simulated results as pseudo-experimental data. The study shows that the proposed optimization methods can identify SMA parameters in an automated fashion using data taken from multiple types of experiment, identifying parameters that fit very closely to the pseudo-experimental data.

Keywords: shape memory alloy, calibration, optimization

INTRODUCTION

Engineers continue to develop innovative structures and products that take advantage of the unique properties of shape memory alloys (SMAs).[1] To support the design of these novel structures, researchers have been developing increasingly accurate constitutive models[2] to predict the complex, non-linear behavior of SMAs over the last several decades. These models, usually implemented using finite element analysis (FEA), are valuable tools for the design of SMA components and structures.[3] However, even with robust models, the response of an SMA structure or actuator under thermomechanical loading cannot be predicted accurately without properly calibrating the model parameters.[4] This calibration procedure is typically carried out using a series of material tests including isothermal/isobaric loading of bulk specimens and differential scanning calorimetry (DSC) on small specimens.[5] The parameters are estimated from these tests using graphical methods. However, identifying the parameters in this manner can be very challenging and lacks objectivity.[6] This study proposes a general framework for automated parameter identification using optimization methods. The framework implementation is demonstrated using two optimization-based parameter identification studies carried out on dog bone FEA models.

The use of automated methods for specific constitutive model calibration, including geologic[7] and steel[8] models, has been investigated in the literature. A series of general methods for automated constitutive model calibration have been proposed that utilize full-field measurements.[9] More recently, the automated calibration of a non-linear SMA constitutive model was carried out using neural networks.[4] In addition, optimization methods have been successfully used to identify model parameters of pseudo-elastic SMA wires.[6] This study presents a general, modular framework for automated SMA parameter identification that works independently of the type or volume of experimental data. We focus on the framework formulation and implementation rather than a specific calibration method in order to provide a highly flexible solution for automated SMA parameter identification.

The first section provides an overview of the automated SMA parameter identification framework and its implementation. The calibration procedure is demonstrated using the geometry of a standard dog bone specimen and "pseudo-experimental data" taken from FEA simulations. Two calibration procedures are conducted: one assuming homogeneous strain and the other using data from a non-homogeneous strain distribution. The second section describes the results of each parameter identification study. The optimized parameters are compared

Behavior and Mechanics of Multifunctional Materials and Composites 2014, edited by Nakhiah C. Goulbourne, Hani E. Naguib, Proc. of SPIE Vol. 9058, 905804
 · doi: 10.1117/12.2046666

with the "ideal" parameters used to generate the pseudo-experimental data. In addition, the error between the data and optimized simulations is investigated. The final section summarizes the results and considers future improvements to and applications of the proposed parameter identification framework.

1. THE PARAMETER IDENTIFICATION FRAMEWORK AND INVERSE PROBLEM FORMULATION

Parameter identification is an inverse problem. Solving this problem (i.e. determining the material parameters that best characterize the material behavior) requires an accurate constitutive model, experimental data, and a solid model reflecting the geometry and loading conditions of the experiment. The model parameters can be iteratively changed until the simulation response matches the experimental results. In order to perform this iterative procedure in an efficient manner, we created an optimization-based parameter identification framework that integrates FEA and a constitutive model to minimize the error between simulations and experimental data. Here, we describe this general framework, its implementation, and the formulation of an "ideal" parameter identification problem using a dog bone FEA model.

1.1 Optimization-Based Parameter Identification Overview

The parameter identification framework uses finite element analysis (FEA) simulations, experimental data, and appropriate design variables to iteratively identify SMA constitutive model parameters. As shown in Figure 1, the framework follows a straightforward methodology. A series of inputs is used to generate one or more FEA simulations that model the experimental setup. The difference, or error, between the simulation results and the provided experimental data is evaluated and converted to a single scalar value. The optimization engine chooses a new set of material parameters based on the error value and the process is repeated until the error is minimized.

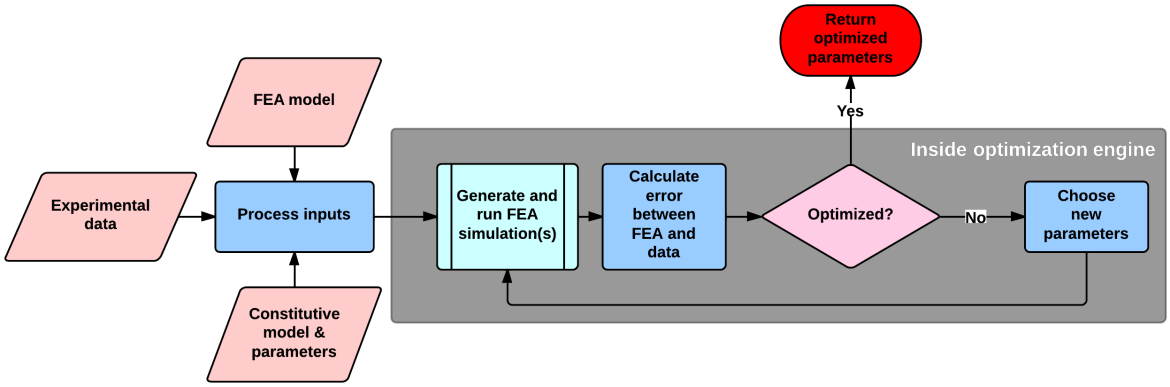

Figure 1. Parameter identification framework flowchart.

In order to calculate the error between an experimental dataset and simulation results, the two sets must be correlated. Figure 2 shows two methods for this procedure. 1D experimental data (e.g. data coming from tensile tests) is compared to simulation results using temporal correlation. In temporal, or time-based, correlation, data is collected at numerous points over time. Each data point reflects the value of some quantity at a single coordinate point or as a homogenous value across part of a specimen. 2D or 3D data, however, must be compared using spatial correlation. With this method, the framework compares experimental digital image correlation (DIC) data with simulation results by comparing components of strain or displacement at different coordinate points on the surface of a specimen. Spatial and temporal interpolation can be used in conjunction, allowing experimental data and simulation results to be compared at multiple points in time and space.

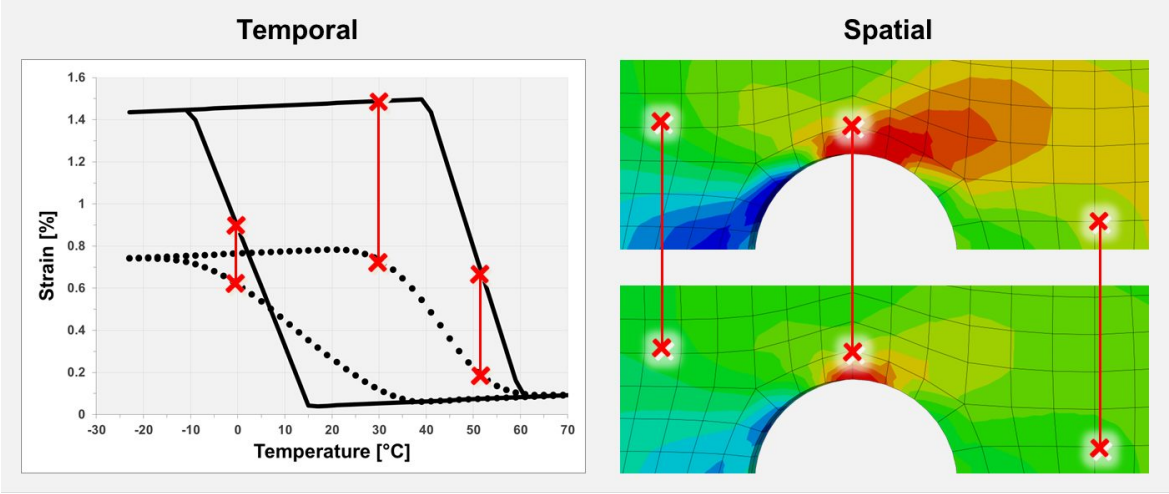

Figure 2. Examples of temporal (left) and spatial (right) correlation.

1.2 Framework Implementation

Implementing the SMA calibration framework requires optimization tools, execution management, structural analysis software, and an accurate constitutive model. We used the Python programming language to integrate each of these components. Python is an open-source, interpreted programming language and is the scripting language of the framework's structural analysis software, making it a natural choice for this project. In addition, there are many well-documented analysis tools written in the Python programming language. The framework takes advantage of the extensive data structures, mathematical functions, and plotting libraries available in the open-source SciPy (Scientific Python) library.[10] In particular, the framework uses the SciPy optimization tools to iteratively minimize the simulation error. We used a SciPy implementation of the sequential least squares quadratic programming (SLSQP)[11] algorithm for all optimization results in this study.

Python scripts automate the iterative calibration process. The framework requires three primary inputs (a structural model, experimental data, and design variables/parameters) to create FEA simulations using the Simulia Abaqus FEA package.[12] The Abaqus/CAE pre-processor opens the inputted model and applies the required thermomechanical loading conditions and current model parameters. Multiple simulations may be required to match all the experimental data sets. After each simulation is generated, the Abaqus/Standard processor executes the analysis. Python scripts interpolate data from the FEA output files and evaluate the error at specified points in time (temporal correlation) and/or space (spatial correlation) by comparing the simulation results with experimental data. The total calculated error is proportional to the root square sum of the error at each point. Finally, after each simulation, the SLSQP minimization algorithm generates a new set of material parameters based on the total error value.

1.3 Finite Element Modeling of a Dog Bone Specimen

As described in the previous section, the first required framework input is a structural model. In order to demonstrate the capabilities of the parameter identification framework, we considered a model of an SMA dogbone specimen used for tensile tests. Typical SMA material characterization studies are only concerned with the homogeneous stress, temperature, or strain measured at the center cross-section of the specimen. The heterogeneous distributions around the loading point are ignored. Our calibration analysis, however, takes into account both the homogenous and non-homogenous regions. Two FEA models were created in Abaqus to represent the regions.

The homogeneous analysis uses a single linear hexahedral element (Abaqus type C3D8) as shown in Figure 3. This model has a distributed pressure load applied on the top face (black) in the x-direction. Boundary conditions prohibit the model from translating or rotating about any axis but do permit deformation in the positive X, Y,

and Z directions. There are three analysis steps: Load, Cool, and Reheat. During the Load step, the model is linearly loaded at 90, 150, or 200 MPa with a constant temperature of 350 K. The model is homogeneously cooled to 250 K and reheated to 350 K during the Cool and Reheat steps, respectively.

A dog bone specimen has two planes of symmetry as illustrated in Figure 3. For this reason, one quarter of the geometry was modeled and discretized using 898 reduced integration quadratic hexahedral elements (Abaqus type C3D20R). As before, boundary conditions prohibit the model from translating or rotating about any axis but do permit deformation in the positive X, Y, and Z directions. There are 12 analysis steps. First, a 100 MPa traction load is applied to one half of the hole's interior surface in the positive x-direction at 350 K. In 20 K increments, the model is homogeneously cooled to 250 K. The model is then homogeneously reheated to 350 K in 20 K increments. Finally, the specimen is unloaded.

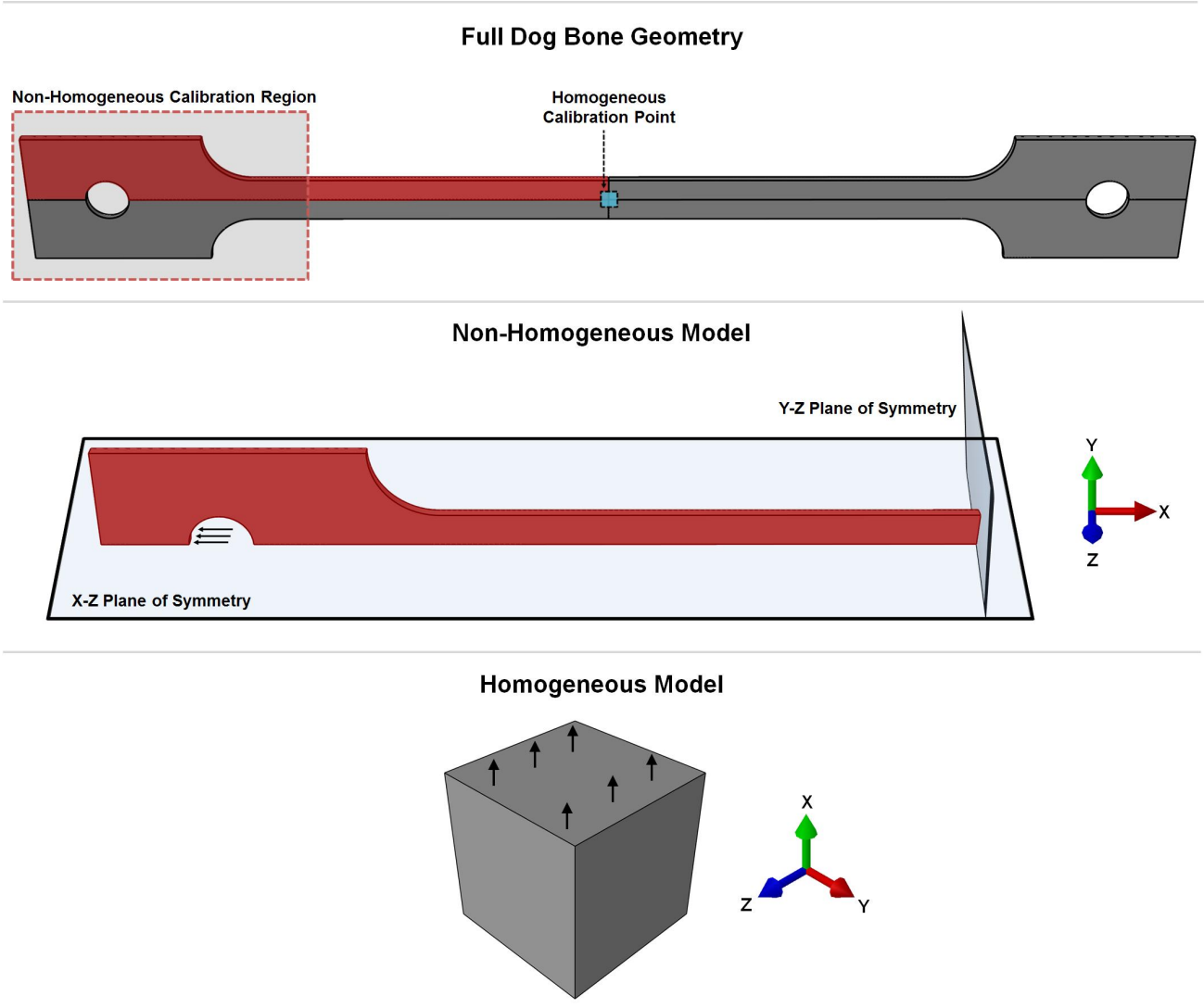

Figure 3. The full dog bone geometry (top) and the simplified models used for analysis (middle and bottom).

1.4 Pseudo-Experimental Data

In this study, we considered an ideal case: the inverse problem is guaranteed to have at least one solution because the "experimental data" perfectly matches a constitutive model when using an unknown set of parameters. This

approach is useful for measuring the performance of the framework under particular inverse problem formulations. There are many factors apart from the experimental data that can influence the final solution including the optimization algorithm, the initial set of inputted parameters (for non-global minimization algorithms), and the distribution of spatial or temporal comparison points. With true experimental data, it may be impossible to establish the absolute best fit of the model to the data. By creating "pseudo-experimental data", however, we can investigate the impact of some of these critical criteria on the inverse problem solution because we know the model parameters that will produce a "perfect fit".[8]

Both of the "dog bone" simulations required a set of pseudo-experimental data. The type and quantity of the pseudo-data for the homogenous and non-homogenous optimizations reflect the type and quantity of data that could be derived from tensile tests and DIC experiments, respectively. Creating pseudo-experimental data for both cases required data generation and data reduction. We generated the data by running both simulations using the constitutive model parameters shown in Table 1. These parameters were chosen because they represent typical SMA model parameters used in the literature.[13] The results of these two simulations represent the "experimentally determined" response of the models to their respective thermomechanical loading conditions.

Table 1. The SMA constitutive model parameters used to generate the pseudo-experimental data.

Property	Value	Property	Value
E^A	90 GPa	$C^A\|_{\sigma=300\ \text{MPa}}$	16 MPa/℃
E^M	63 GPa	$C^M\|_{\sigma=300\ \text{MPa}}$	10 MPa/℃
$v^A = v^M$	0.33	$H_{t,max}$	0.0158
$\alpha^A = \alpha^M$	10×10^{-6} ℃	$H_{t,min}$	0.0
ΔM_s	35 ℃	σ_{crit}	12 MPa
M_f	-31 ℃	k_t	0.0075
A_s	15 ℃	n_1, n_2, n_3, n_4	0.6, 0.2, 0.2, 0.3
A_f	69 ℃	σ_{cal}	300 MPa

The homogeneous results were reduced into three strain vs. temperature curves as shown in Figure 4. For each curve, the strain in the loading direction (ϵ_{xx}) was interpolated at 102 evenly-spaced temperature points. The 102 points were interpolated from the original set of 100 frames in the cooling and heating analysis steps. 102 points were chosen in order to capture all the features of the strain-temperature curve.

The non-homogeneous results were reduced into 11 distributions of three components: ϵ_{xx}, ϵ_{yy}, and ϵ_{xy}. These three in-plane strain distributions are representative of data that could be obtained from 2D DIC experimental data. Each of the 11 distributions correspond to one of the eleven cooling and heating analysis steps in the simulation. Thus, the strain distributions were recorded in intervals of 20 K. These 11 frames adequately sampled the full thermomechanical loading spectrum of the simulation. At each temperature interval (or frame), the values of ϵ_{xx}, ϵ_{yy}, and ϵ_{xy} were saved for 80 coordinate points. The 80 spatial points are distributed throughout the surface of the 3D model as illustrated in Figure 4. It is important that the points be representative of as much of the strain distribution as possible.

2. ANALYSIS AND RESULTS

The FEA models and generated pseudo-experimental data were put into the SMA calibration framework. Two optimization-based calibrations were conducted: one for the homogeneous region and the other for the non-homogeneous region. Each calibration procedure optimized a subset of the constitutive model parameters described in Table 1. In this section we present the results of the optimization studies, highlighting both the optimized parameters and their corresponding simulations.

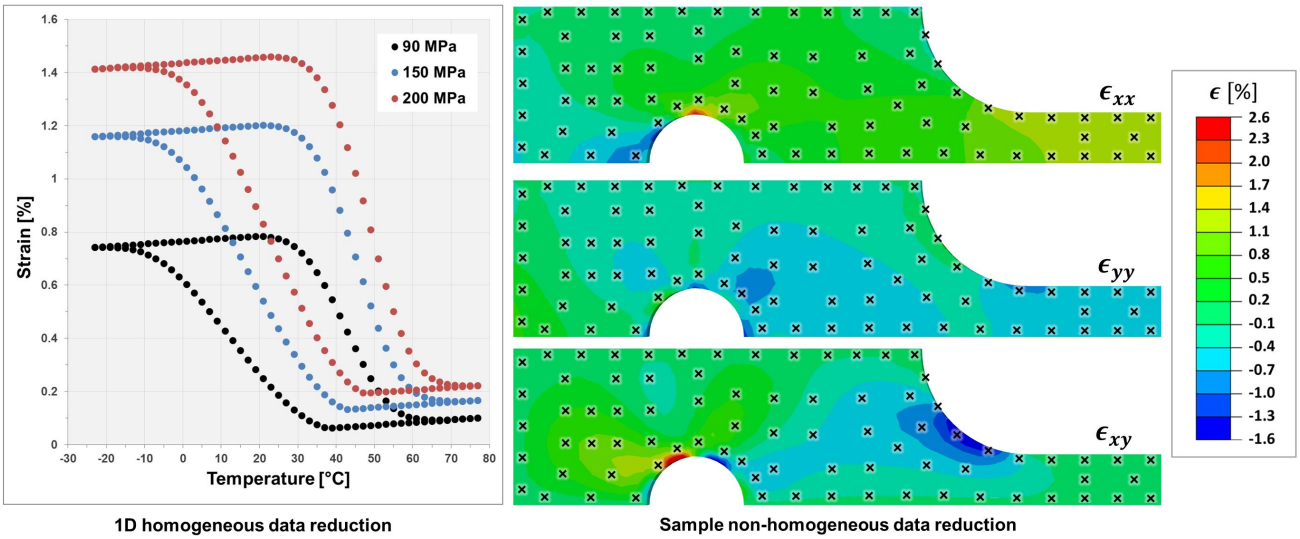

Figure 4. Pseudo-experimental data sets used in the dog bone parameter identification. The homogeneous results were interpolated at 102 temperature points for each of the three applied pressures (left). Non-homogeneous results for ϵ_{xx}, ϵ_{yy}, and ϵ_{xy} were recorded at 80 points from 11 temperature frames. The distributions at the lowest applied temperature (250K) are shown here (right).

2.1 Optimization Input Variables

The 12 parameters shown in Table 2 were selected for optimization. All remaining model parameters were set as specified in Table 1. It was assumed that these parameters, including E^A and E^M, could easily be evaluated from the experimental data. The SLSQP method is a gradient-based algorithm. As such, it requires an initial guess for the model parameters. The initial guess parameters are provided in Table 2. These parameters were chosen as relatively "standard" values for the model parameters and could be used a starting point for calibrating a variety of actuation experiments. In addition, bounds were placed on each parameter in order to avoid meaningless results and simulations. Note that the parameters M_s, A_s, and A_f were replaced with ΔM_s, ΔA_s, and ΔA_f, respectively, where $\Delta M_s = M_s - M_f \geq 0$, $\Delta A_s = A_s - M_f \geq 0$ and $\Delta A_f = A_f - A_s \geq 0$. Values of ΔM_s, ΔA_s, and ΔA_f below zero violate assumptions made by the SMA constitutive model. Defining the three optimization variables in this way ensures that these constraints will not be violated.

Table 2. The initial values and bounds for the optimized parameters.

Parameter	Initial Value	Low-Bound	High-Bound
ΔM_s [°C]	25	0.5	50
M_f [°C]	-15	-40	50
ΔA_s [°C]	50	0.5	80
ΔA_f [°C]	20	0.5	80
$C^A\|_{\sigma=300\ \text{MPa}}$ [MPa/°C]	7	4	25
$C^M\|_{\sigma=300\ \text{MPa}}$ [MPa/°C]	7	4	25
$H_{t,max}$	0.03	0.01	0.08
k_t	0.008	0.001	0.015
n_1 , n_2 , n_3 , n_4	1	0.2	1

2.2 Parameter Identification Results

The homogeneous model and reduced pseudo-data sets were put into the automated SMA-calibration framework. Using the initial guess model parameters shown in Table 2, the simulation corresponded relatively poorly to the

representative data sets with a root-mean-square deviation of 0.619% strain. Running the parameter identification framework returned material parameters that fit the pseudo-data sets much better with a root-mean-square deviation of 0.0124% strain. Thus the error was diminished by a factor of 50. Figure 5 shows the initial and optimized simulation results overlaid onto the reduced pseudo-data sets. Although the automated calibration procedure returned model parameters that correlate very well to the pseudo-data, the optimized simulation is not a "perfect fit." Table 3 shows the optimized parameters that were determined during the homogeneous calibration procedure. Many of these parameters differ from the "ideal" parameters used to generate the pseudo-data.

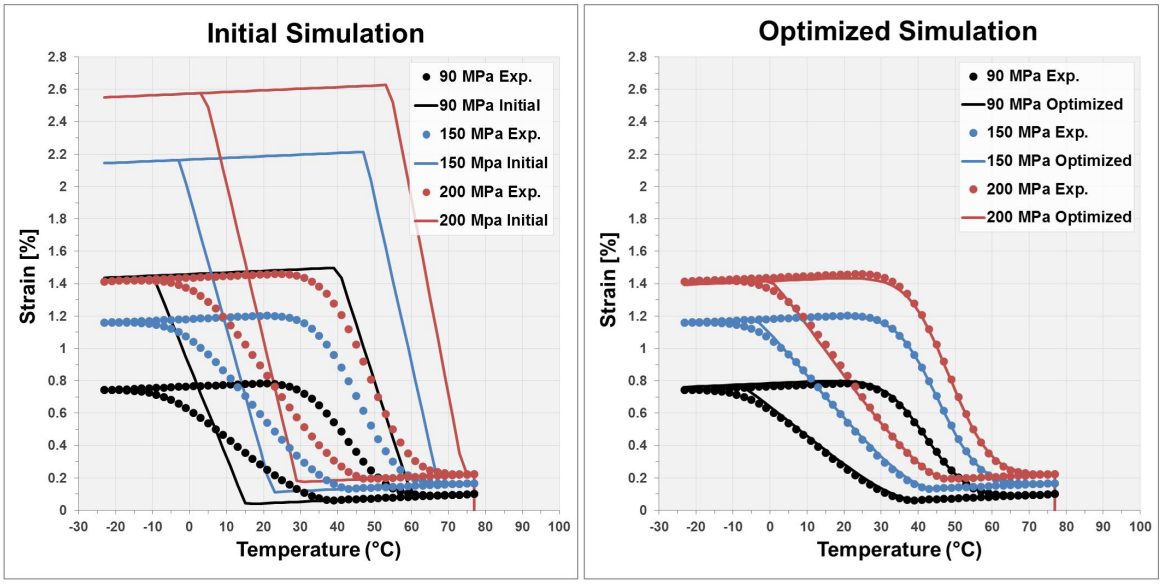

Figure 5. A simulation run with the initial guess set of parameters (left) compared with a simulation run with the optimized homogeneous parameters (right).

Table 3. The SMA constitutive model parameters used and identified in various stages of analysis. The pseudo-experimental data was generated using the parameters in column 2. All optimizations started with the same initial parameters (column 3). The parameters returned after the homogeneous and non-homogeneous optimizations are shown in columns 4 and 5, respectively.

	Ideal	**Initial Guess**	**Homogeneous**	**Non-Homogeneous**
Parameter	Value	Value	Value	Value
M_s [°C]	35	10	35.8	26.1
M_f [°C]	-31	-15	-11.7	-23.6
A_s [°C]	15	35	8.66	14.7
A_f [°C]	69	55	71.2	50.2
$C^A\|_{\sigma=300\ \mathrm{MPa}}$ [MPa/°C]	16	7	16.1	8.18
$C^M\|_{\sigma=300\ \mathrm{MPa}}$ [MPa/°C]	10	7	11.5	7.93
$H_{t,max}$	0.0158	0.03	0.0146	0.0141
k_t	0.00752	0.008	0.00868	0.00872
n_1	0.6	1	0.557	0.830
n_2	0.2	1	0.845	0.286
n_3	0.2	1	0.201	0.912
n_4	0.3	1	0.200	0.261

The non-homogenous FEA model and reduced pseduo-data were also put into the parameter identification framework. The full set of non-homogeneous experimental data consists of strain distributions for three compo-

nents: (ϵ_{xx}, ϵ_{yy}, and ϵ_{xy}) at 11 homogeneous temperatures. The large number of comparison values (80 spatial points, 3 strain components, and 11 temperatures yields 2640 comparison values) makes it difficult to portray the full set of data. For these reasons, only the strain distribution in the loading direction (ϵ_{xx}) at the minimum temperature (250 K) will be depicted and analyzed in this study. At 250 K, the specimen has fully transformed into martensite and experiences the highest strain. Thus, the constitutive model parameters have a very high impact on the strain distribution at this temperature, making it an ideal point of comparison.

As before, the "initial guess" parameters given in Table 2 did not correspond well to the ϵ_{xx} distribution at 250 K and had a root-mean-square deviation of 0.211% strain. The optimization-based calibration procedure returned parameters that better matched the desired response. The simulation with the optimized parameters had a root-mean-square deviation of 2.00×10^{-3} percent strain, nearly 100 times lower than the original.

Figure 6 shows the ϵ_{xx} strain distributions simulated using the "initial guess" parameters and optimized parameters compared with the pseudo-experimental results. This same data was reduced and plotted in Figure 7. In this plot, each comparison point index refers to one of the spatial points at which the simulation results were compared with the representative experimental data. On this plot, the indexes were arranged in increasing order by the their respective x-coordinates. The absolute difference, or error, between the simulation and the pseudo-data is plotted on the y-axis.

As with the homogeneous optimization, the optimized simulation does not perfectly match the pseudo-experimental data. Table 3 shows the optimized parameters that were determined during the non-homogeneous calibration procedure. As before, many of these parameters differ from the "ideal" parameters used to generate the pseudo-data.

The results of both parameter identification studies yield the following conclusions:

1. Because the parameters of the SMA constitutive model used in this study are highly coupled, it is possible that multiple sets of parameters could be used to accurately characterize the material response.

2. The parameter identification framework may not return the "global" solution if a non-global optimization algorithm is used. In addition, the solution may be dependent on the initial conditions.

3. Even with a non-global optimization algorithm, the parameter identification framework returned parameters that correlate very well to a set of experimental data (or, in this case, pseudo-data derived from simulation results) for both optimization studies.

2.3 Comparison Between Homogeneous and Non-Homogeneous Calibration Results

In this study, the parameters that best characterized the pseudo-experimental data were known (because they were used to generate the data sets) and were the same for both the homogeneous and non-homogeneous cases. However, if "true" experimental data sets would have been used, it is unlikely that similar sets of parameters would have best characterized both the homogeneous and non-homogeneous data due to the effects of anisotropy.

The use of pseudo-experimental results in place of actual experimental data limits the scope of comparison between the parameters identified by the two optimization studies. However, comparing the magnitude of the absolute error at each comparison point for both sets of parameters does yield some useful insight. Figure 8 repeats the error distribution among the comparison points that was first illustrated in Figure 7. In this plot, however, the error distribution is compared with the error in simulating the model with the optimized-homogeneous parameters. Note the large change in scale of the y-axis. For most comparison points, the non-homogeneous optimization parameters resulted in a simulation that better matched the desired behavior. Notable exceptions, however, are the coordinate points that lie on the homogeneous part of the specimen. These points are clearly better represented by the parameters resulting from the homogeneous optimization. Although the absolute difference in strain is small for this "ideal" case, it would likely be more pronounced in "true" experimental data. Therefore, it is very important to consider the impact of the comparison point distribution on the results of the calibration process.

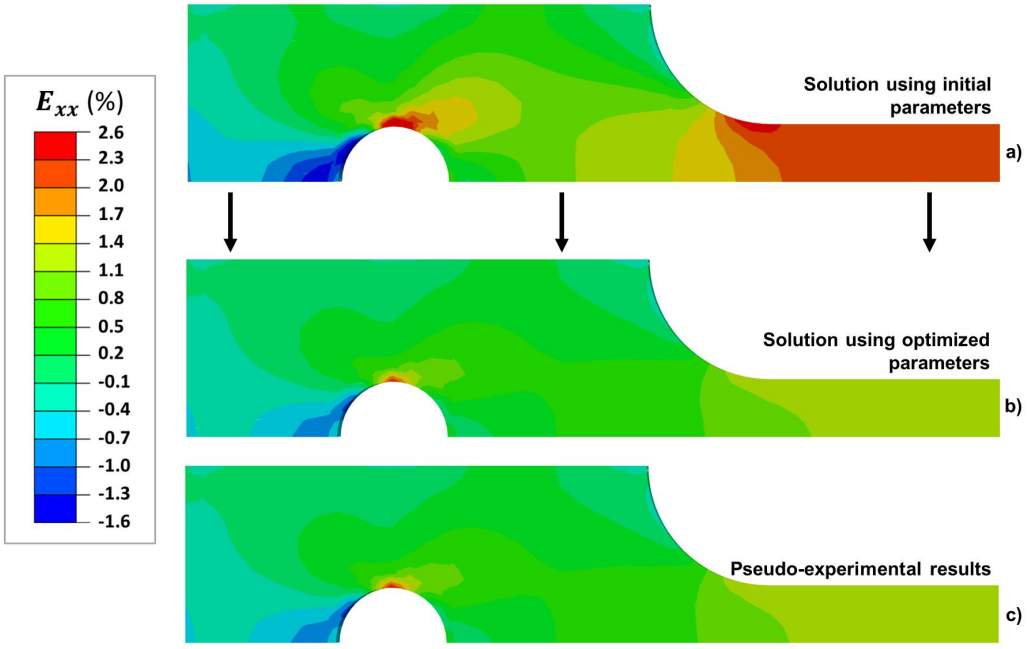

Figure 6. The ϵ_{xx} distributions on a portion of the 3D dog bone model using the set of guess parameters (a), the non-homogeneous optimized parameters (b), and the "ideal" parameters.

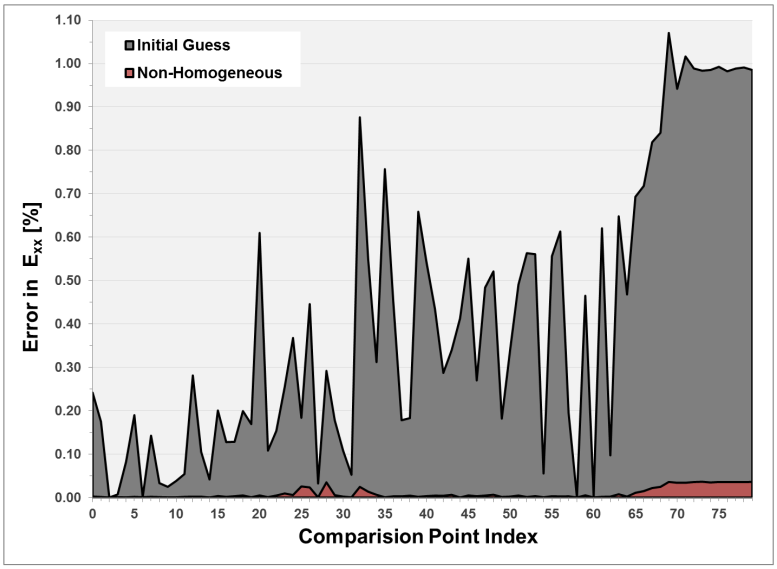

Figure 7. 80 coordinate points were used as points of comparison on one surface of the 3D dog bone model. This plot shows their absolute error before and after material parameter optimization.

3. CONCLUSION

An automated parameter identification framework was developed in order to iteratively determine the constitutive model parameters of shape memory alloys based on 1D or 2D experimental data. The Python-based framework correlates experimental data with simulation results and outputs a scalar error value proportional to the root square sum of the difference at each comparison point. This error is minimized by iteratively changing the material parameters. In order to test the framework's capabilities, an "ideal" inverse problem was formu-

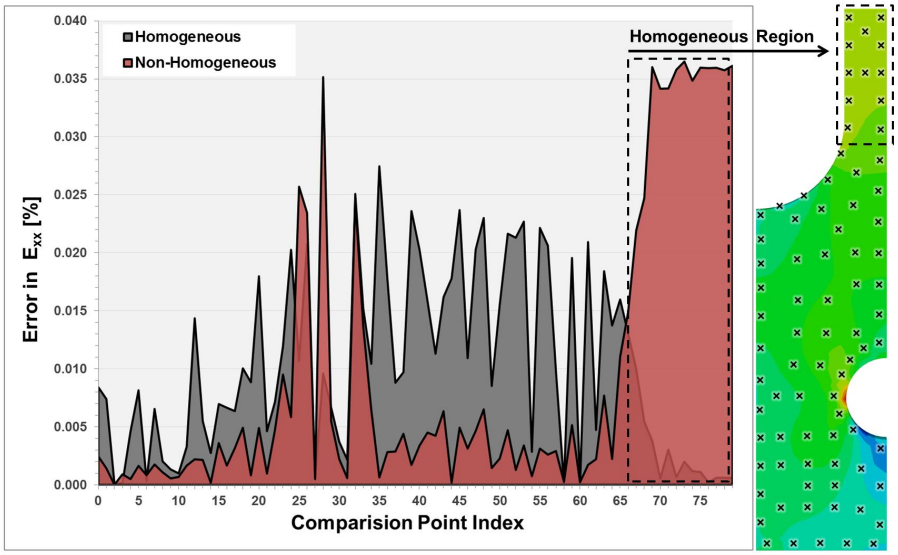

Figure 8. 80 coordinate points were used as points of comparison on one surface of the 3D dog bone model. This plot shows the relative simulation error with respect to the pseudo-experimental data when parameters derived from the homogeneous optimization and non-homogeneous optimization methods were used.

lated using "pseudo-experimental data." The pseudo-data was generated and reduced from two dog bone FEA simulations produced using a known set of constitutive model parameters. Two optimization-based calibration procedures were conducted: the first determined the material parameters using a simulation with a homogeneous strain distribution while the second concentrated on a non-homogeneous region.

The homogeneous and non-homogeneous calibrations significantly reduced the simulation error. However, neither set of optimized parameters closely matched the "ideal" set of parameters used to generate the pseudo-experimental data. These differences are likely due to the non-global optimization algorithm and the initial guess. With a more robust optimization algorithm, the parameter identification framework could become a highly flexible tool for objective SMA characterization, allowing creative and high-throughput experiments to be used in place of traditional methods.

REFERENCES

[1] Morgan, N., "Medical shape memory alloy applications-the market and its products," *Materials Science and Engineering: A* **378**(12), 16 – 23 (2004). European Symposium on Martensitic Transformation and Shape-Memory.

[2] Hartl, D. J., Mooney, J. T., Lagoudas, D. C., Mabe, J. H., and Calkins, F. T., "Experimentally validated numerical analysis of aerostructures incorporating shape memory alloys," (2008).

[3] Burton, D., Gao, X., and Brinson, L., "Finite element simulation of a self-healing shape memory alloy composite," *Mechanics of Materials* **38**(56), 525 – 537 (2006).

[4] James V. Henrickson, Kenton Kirkpatrick, J. V., "Characterization of shape memory alloys using artificial neural networks," (2009).

[5] Hartl, D. and Lagoudas, D., "Thermomechanical characterization of shape memory alloy materials," in [*Shape Memory Alloys: Modeling and Engineering Applications*], Lagoudas, D., ed., ch. 2, 53–119, Springer-Verlag, New York (2008).

[6] Meraghni, F., Chemisky, Y., Piotrowski, B., Echchorfi, R., Bourgeois, N., and Patoor, E., "Parameter identification of a thermodynamic model for superelastic shape memory alloys using analytical calculation of the sensitivity matrix," *European Journal of Mechanics - A/Solids* **45**(0), 226 – 237 (2014).

[7] Pal, S., Wathugala, G. W., and Kundu, S., "Calibration of a constitutive model using genetic algorithms," *Computers and Geotechnics* **19**(4), 325 – 348 (1996).

[8] Fedele, R., Filippini, M., and Maier, G., "Constitutive model calibration for railway wheel steel through tensiontorsion tests," *Computers Structures* **83**(1213), 1005 – 1020 (2005).

[9] Avril, S., Bonnet, M., Bretelle, A.-S., Grdiac, M., Hild, F., Ienny, P., Latourte, F., Lemosse, D., Pagano, S., Pagnacco, E., and Pierron, F., "Overview of identification methods of mechanical parameters based on full-field measurements," *Experimental Mechanics* **48**(4), 381–402 (2008).

[10] Oliphant, T. E., "Python for scientific computing," *Computing in Science and Engineering* **9**(3), 10 – 20 (2007).

[11] Kraft, D., "A software package for sequential quadratic programming," Tech. Rep. DFVLR-FB 88-28, DLR German Aerospace Center-Institute for Flight Mechanics, Koln, Germany (1988).

[12] Abaqus, *Analysis User's Manual*. Dassault Systèmes of America Corp., Woodlands Hills, CA (2010).

[13] Hartl, D. J., Mooney, J. T., Lagoudas, D. C., Calkins, F. T., and Mabe, J. H., "Use of a Ni60Ti shape memory alloy for active jet engine chevron application: II. experimentally validated numerical analysis," *Smart Materials and Structures* **19**(1), 015021 (2010).